that is likely to contain the Tommotian/Atdabanian boundary. More precise correlation of this excursion with the base of the Atdabanian, as suggested by Tucker[8], cannot be achieved using the fossils that have so far been discovered here as none of them is exclusively Tommotian. A profile through the basal Cambrian of the Australian Flinders Ranges[31] reveals a positive $\delta^{13}C$ excursion near the first appearance of archaeocyaths within the Atdabanian, which may correlate with the upper Tiout $\delta^{13}C$ excursion in the Calcaire Supérieur. Further correlation of this excursion at Tiout is not yet possible, because other $\delta^{13}C$ profiles through Tommotian and Atdabanian parts of Precambrian/Cambrian boundary sequences have not been reported.

These new microfossil and trace fossil data for the Tiout sequence, together with the re-calibrated isotope curve, identify the position of the Precambrian/Cambrian boundary about 1,000 m lower than was previously generally recognized[1], and they require revision of correlations of $\delta^{13}C$ profiles, assuming that these reflect global changes. The generally light $\delta^{13}C$ values throughout the Série Lie de Vin[8] cannot now be correlated with light values in the Vendian of other sections[4,5] but correspond instead with light $\delta^{13}C$ in the Tommotian of Australian[31]. As the quest for a Precambrian/Cambrian boundary stratotype increasingly combines chemical and physical methods of correlation (including magnetostratigraphy and radiometric dating, as well as stable isotopes) with palaeontological information, thick carbonate sequences across the boundary, of which the Dolomie Inférieure of the northwestern Anti-Atlas is a prime example, are likely to assume increasing importance despite their relatively limited potential for biostratigraphy alone. □

Received 17 November 1989; accepted 23 February 1990.

1. Cowie, J. W. & Brasier, M. D. *Oxford Monogr. Geol. Geophys.* **12** (Clarendon, Oxford, 1989).
2. Cowie, J. W. *Episodes* **8**, 93–97 (1985).
3. Veizer, J., Holser, W. T. & Wilgus, C. K. *Geochim. cosmochim. Acta* **44**, 579–587 (1980).
4. Knoll, A. H., Hayes, J. M., Kaufman, A. J., Swett, K. & Lambert, I. B. *Nature* **321**, 832–838 (1986).
5. Magaritz, M., Holser, W. T. & Kirschvink, J. L. *Nature* **320**, 258–259 (1986).
6. Aharon, P., Schidlowski, M. & Singh, I. B. *Nature* **327**, 699–702 (1987).
7. Lambert, I. B., Walter, M. R., Wenlong, Z., Songnian, L. & Guogan, M. *Nature* **325**, 140–142 (1987).
8. Tucker, M. E. *Nature* **319**, 48–50 (1986).
9. Latham, A. J. & Riding, R. *Proc. Int. Ass. Sedim. Eur. Meet.* Leuven 127–128 (Int. Ass. Sedim., 1988).
10. Choubert, G. *Congr. Geol. Int. 19e, Alger, Monogr. region* **6**, 77–194 (1952).
11. Schmitt, M. O. & Monninger, W. E. W. in *Fossil Algae* (ed. Flügel, E.) 80–85 (Springer, Berlin, 1977).
12. Monninger, W. E. W. *Arb. Paläont. Inst. Würzburg* **1**, 1–289.
13. Debrenne, F. *Notes & M. Serv. géol. Maroc* **179**, 1–265 (1964).
14. Debrenne, F. & Debrenne, M. *Geol. Mag.* **115**, 101–119 (1978).
15. Sdzuy, K. *Geol. Mag.* **115**, 83–94 (1978).
16. Hupé, P. *Centre natn. Rech. sci. Paris* **76**, 163 (1958).
17. Schmitt, M. O. *Arb. Paläont. Inst. Würzburg* **2**, 1–188 (1979).
18. Choubert, G., Faure-Muret, A. & Timofeiev, B. K. *C. r. hebd. Séanc. Acad. Sci. Paris* **288D**, 191–194 (1979).
19. Rozanov, A. Yu. *Tr. Akad. Nauk SSSR* **206**, 102–104 (1969).
20. Bertrand-Sarfati, J. *Newslett. Stratigr.* **10**, 20–26 (1981).
21. Houzay, J-P. *Géol. Méditerr.* **6**, 379–384 (1979).
22. Leblanc, M. in *Earth's Pre-Pleistocene Glacial Record* (eds Hambrey, M. J. & Harland, W. B.) 120–122 (Cambridge University Press, 1981).
23. Mifdal, A. & Peucat, J-J. *Sci. Géol., Bull.* **38**, 185–200 (1985).
24. Riding, R. & Voronova, L. in *Paleoalgology* (eds Toomey, D. F. & Nitecki, M. H.) 56–78 (Springer, Berlin, 1985).
25. Riding, R. & Voronova, L. *Geol. Mag.* **121**, 205–210 (1984).
26. Crimes, T. P. *Geol. Mag.* **124**, 97–119 (1987).
27. Fairchild, I. J., *28th Int. Geol. Congr., Washington 1989. Abstr. 1:* 470 (1989).
28. Schidlowski, M., Eichmann, R. & Junge, C. E. *Geochim. cosmochim. Acta* **40**, 449–456 (1976).
29. Fairchild, I. J. & Hambrey, M. J. *Precambrian Res.* **26**, 111–168 (1984).
30. Hsu, K. J. *et al. Nature* **316**, 809–811 (1985).
31. Tucker, M. E. *Terra Nova* **1**, 573–582 (1990).

ACKNOWLEDGEMENTS. We thank P. Aharon, M. Brasier, J. Cowie, F. Debrenne and M. Tucker for helpful comments on the manuscript, P. Crimes for trace fossil identifications, and the Ministère de l'Energie et des Mines, Rabat, for permission to work in Morocco. A.L.'s work was supported by NERC.

Bounds on global dynamic topography from Phanerozoic flooding of continental platforms

Michael Gurnis

Department of Geological Sciences, University of Michigan, Ann Arbor, Michigan 48109-1063, USA

THE movement of continents with respect to a large-scale pattern of dynamic topography and geoid, imposed by convection in the mantle, must contribute to the flooding of continental platforms. Here I investigate this phenomenon, using a one-dimensional model in which a continent moves from a high to a low of dynamic topography (and geoid), and in the process is partially exposed and then flooded. If the dynamic topography is greater than about 150 metres, the model continent is flooded by more than 30%—the maximum amount of flooding experienced by North America during the entire Phanerozoic eon[1]. The model suggests that a large-scale pattern of dynamic topography must have an amplitude of less than 150 metres, and that the admittance, the ratio of geoid to dynamic topography, may be greater than 0.3. Recent models of global mantle dynamics[2,3] which predict the long-wavelength geoid from mantle seismic structure are apparently inconsistent with Phanerozoic flooding.

After the acceptance of plate tectonics, it was noted that the late Cretaceous marine transgression onto the continents was correlated with the 'volume' of oceanic ridges[4]. This led to the hypothesis that when spreading rates and/or length of ridges increase, ocean basins become more shallow and sea level rises[5]. This is unlikely to be the only type of control exerted by the mantle and tectonic plates on long-term eustatic sea-level fluctuations, because density anomalies in the deep mantle (the existence of which is revealed by anomalies in seismic travel times[3,6,7], could have caused the continents to bob up and down as they drifted around the surface of the Earth. For a model that is consistent with the observed geoid, long-wavelength density variations inferred from body-wave seismic tomography give rise to global-scale variations in dynamic topography on the order of one kilometre[2,3]. Recently, Cazenave *et al.*[8] were able to extract a global residual topography, of ~300 m amplitude, by correcting for shallow density variations in the lithosphere. These corrections include the removal of contributions due to cooling of the oceanic lithosphere with increasing age[9] and the subtraction of a mean baseline for stable continental platforms. The residual topography is dominated by a degree-two pattern which is strongly correlated with the geoid[8].

Another approach to constraining dynamic topography arises from the effect on sea level of the continental "bobbing" described above: by requiring continental flooding to be less than the observed areal coverage of marine deposits, an upper bound can be placed on the magnitude of dynamic topography. In the one-dimensional model used here, a continent is moved over a surface that has a dynamic topography comprised of a single wavelength. Because of the ambiguity in the data, however, essentially any wavelength will result in periodic flooding; here I am concerned only with wavelengths larger than the scale of continents. In this model, dynamic topography, H, and geoid, N, vary as $H_0 \sin 2\pi x$ and $N_0 \sin 2\pi x$ respectively. Here x is non-dimensional and varies between 0 and 1. The admittance, Z, is defined as N_0/H_0. I have used three values of N_0: 0, 50 and 100 m; in comparison, the degree-two and order-two geoid deduced in ref. 2 is ~50 m. The continental crust has a thickness W_c which is symmetrical about its centre at x_c. Two types of crustal thickness variations were used, one leading to a linear hypsometry and the other leading to the average present-day continental hypsometry[10] (solid circles, Fig. 1); the latter is hereafter referred to as the 'world' hypsometry data set. The present range in continental hypsometric curves is indicated in Fig. 1 as the shaded area surrounding the 'world' data set. The total height variation for the linear hypsometric type of continent is h_c. The centre of the continent is moved from the peak of dynamic topography at $x = 0.25$ to the minimum at $x = 0.75$. At each value of x, a constant volume of water is placed on the

system. Starting from the topographically lowest point, water is added to the system such that each mass column is in isostatic equilibrium with respect to the dynamic topography; the water surface follows the shape of the geoid. The system was solved by isostatically balancing columns made up of water, crust and mantle with densities of 1,000, 2,700 and 3,300 kg m^{-3} respectively. For models with linear hypsometries, the volume of water added was such that the continent was flooded by 50% ($f_c = 0.50$) when $N_0 = 0$ and $Z = \infty$; this corresponds to a flat water surface with no dynamic topography. For models with the average observed hypsometry, f_c was taken to be 0.18—the average fraction by which North America was flooded over the Phanerozoic[1]—when $N_0 = 0$ and $Z = \infty$. Flooding minima and maxima occur over the lowest and highest points in the geoid, for any Z. The fractional change of continent flooded, Δf_c, is defined as the absolute difference in flooding between $x_c = 0.25$ and $x_c = 0.75$. Results are shown in Fig. 2 for the case with 'world' hypsometry, $Z = 0.5$, and $N_0 = 100$ m for $x_c = 0.25$ (top) and 0.75 (bottom). Although the continent is resting at the geoid high at $x_c = 0.25$, it is more exposed than at $x_c = 0.75$ because the dynamic topography has twice the amplitude of the geoid and thus 'pushes' the continent above the sea surface. The change in flooding (Δf_c) between these two cases is 0.26 and the mean flooding is 0.18.

Flooding is strongly influenced by the admittance and the geoid, as summarized in Fig. 3. For a model Earth with little or no dynamic topography (large Z) and a non-zero geoid, the continent is flooded more extensively at the geoid high than at the geoid low. As the admittance diminishes and the amplitude of dynamic topography increases, progressively less flooding occurs over the geoid high and progressively more over the geoid low. When $Z = 1$, the effects of flooding at the geoid high and exposure at the topographic high cancel as the continent moves from geoid high to low; this corresponds to the minimum in the curve of Z against Δf_c in Fig. 3. As Z falls below unity, the amplitude of dynamic topography increases, Δf_c increases, and the continent becomes more exposed at the geoid high and more flooded at the geoid lows (compare Fig. 2). If the 'world' hypsometry is used (dotted line *a* in Fig. 3), the range of flooding exceeds 0.30 when Z falls below ~0.45 (for $N_0 = 100$ m). North America (the only platform for which a reasonably complete flooding record is available) experienced a maximum flooding range of 30% over the Phanerozoic[1]. When the amplitude of dynamic topography is greater than ~200 m, flooding in the model is inconsistent with that observed. If N_0 is decreased to 50 m, the amount of flooding also decreases for a given Z (dashed line *b* in Fig. 3); the flooding exceeds 30% when the admittance is less than 0.3. Finally, if there is no geoid ($Z = 0$), the maximum permissible flooding is exceeded when $H_0 >$ 110 m. Given that the true geoid should lie in the range 0–100 m, the model strongly suggests that the amplitude of large-scale

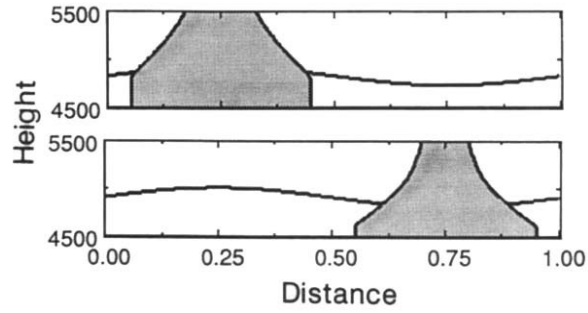

FIG. 2 Total topography and sea surface for the case $Z = 0.5$ and $N_0 = 100$ m at $x_c = 0.25$ (top) and 0.75 (bottom). The topography of the continent (shaded) is the result of isostatic topography (caused by crustal thickness variations), dynamic topography and sea-water loading. The continent becomes more flooded when positioned over a dynamic topography and geoid low. The original hypsometry, without dynamic topography and water loading, would follow the observed hypsometry (the 'world' data set) as shown in Fig. 1. Elevations above 5,500 m have been truncated.

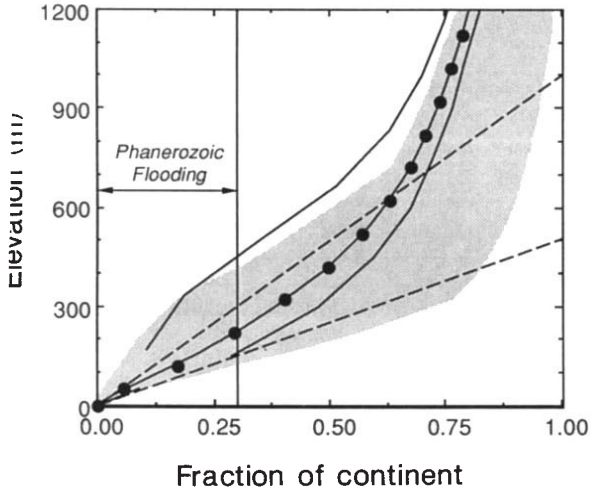

FIG. 1 Observed and calculated hypsometries. The horizontal axis is the fraction of continental area below a given elevation. Solid circles denote the 'world' data set of Harrison *et al.*[10]; this is the average of all present-day continents. The extremes of this data set are indicated by the shaded area; the upper edge is defined by the hypsometric curves for Africa and Asia, and the lower by Europe. The area below sea level has been corrected for sea-water loading; the curve has been shifted such that the minimum is at the origin. The data set was fitted with a fifth-order polynomial (solid curve passing through the solid circles) which was then used in the calculations. In the models, the hypsometry is also influenced by dynamic topography, and the extreme variations are shown by the solid lines bounding the 'world' average for a case with $Z = 0.5$ and $N_0 = 100$ m (see text). The dashed curves are two linear hypsometries. The observed range in the fraction of North America flooded over the entire Phanerozoic[1] is also indicated.

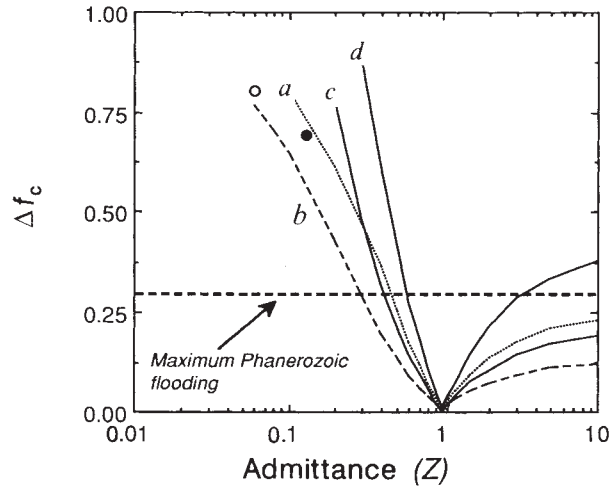

FIG. 3 Total range in fraction of continent flooded, Δf_c, versus admittance, Z, for two cases with the 'world' hypsometry of Harrison *et al.*[10]. Curve *a* is for $N_0 = 100$ m and curve *b* is for 50 m. The two solid curves are for the linear hypsometries shown in Fig. 1: *c* with $h_c = 1{,}000$ m and *d* with $h_c =$ 500 m. The 'Maximum Phanerozoic flooding' curve corresponds to the range of flooding that North America experienced during the Phanerozoic[1]. In all models, $w_c = 0.4$ (approximately the ratio of continental area (plus their margins) divided by the surface area of the Earth). Two specific spherical dynamic models that predict the observed geoid have been explored: the solid circle denotes model CC-U10 from ref. 2 and the open circle denotes model W4 from ref. 3; both models assume whole-mantle convection with a moderate increase in viscosity from upper to lower mantle.

dynamic topography is $<150 \pm 50$ m. In addition, I have studied two specific cases from the work of Hager *et al.*[2,3], where the geoid is calculated using mantle density anomalies resolved through seismic tomography; as discussed above, these models have about 600–1,000 m of dynamic topography and predict flooding (Fig. 3, circles) in excess of 70%—inconsistent with the extent of observed marine deposits.

Flooding is also influenced strongly by hypsometry; this is demonstrated in Fig. 3, where curves *a*, *c* and *d* differ only in respect to their intrinsic hypsometries. Steeper platform hypsometries (larger h_c) result in smaller Δf_c for a given Z. Hypsometries evolve[11,12] as continents are subjected to different tectonic environments at their margins, such that platform slope varies amongst the continents. With the exception of Africa, the variation is at present less than a factor of two[11]. An uncertainty of this magnitude is represented by the solid lines in Fig. 3: the minimum permissible admittance decreases from 0.55 to 0.40 when platform slope is increased by a factor of two. If the intrinsic variation in average hypsometry over the Phanerozoic has been as great as the present variation between continents[12], the bound on Z should vary only by about ± 0.1 if Z is in the range 0.3–0.5. But such variations in hypsometry are accounted for implicitly because the total continental hypsometry varies as the continent moves over the undulations in dynamic topography. This variation is shown for a particular model ($Z = 0.5$ and $N_0 = 100$ m) in Fig. 1 as the solid lines that bound the 'world' hypsometry (solid circles). This variation can be as large as the variation currently observed in the hypsometries between individual continents (shaded area in Fig. 1), and even the slope of the steepest platform (Africa) can be exceeded by the total modelled hypsometry.

The upper bound on a large-scale pattern of dynamic topography is dependent on three fundamental assumptions. (1) The flooding record of North America is representative of all continents. (2) The observed flooding represents the maximum areal coverage of inland seas. (3) A continent experienced complete excursions from a dynamic topography high to a low at least once during the Phanerozoic. Although the flooding-record compilations are not as complete as those for North America, only China (individually) has flooded by significantly more than 30% (ref. 11). If all continents are averaged together, the data summarized by Algeo and Wilkinson[11] shows that the average flooding at any given time did not exceed 30%. Because marine deposits are eroded during exposure[1] and rapid transgressive/regressive cycles may not have had time to leave recognizable deposits, the observation of the fraction of platform now covered with marine deposits may not supply an upper bound on flooding. This ambiguity is unavoidable given our understanding of continental stratigraphy. Complete excursion from dynamic topography high to low is a reasonable assumption given that most continents have apparently moved from a geoid high to a geoid low over the last 150 Myr following the breakup of Pangea[13]. In addition, recent theoretical modelling of plate-mantle interaction shows that continental plates consistently make complete excursions from dynamic topography highs to lows[14,15].

The models explored here purposely neglect other sources of large-amplitude sea level fluctuations, the most important being variations in oceanic ridge spreading. Incorporation of other mechanisms probably would only tend to increase the range of flooding—the estimated bound on the admittance remains a lower one. The effect on flooding history of restricting the motion of a single continent to one dimension is uncertain, and can be addressed only by moving continental and oceanic plates with their observed palaeo-positions over the surface of a sphere with different admittances and dynamic topographies. Comparison of such models with the observed spatial patterns of marine deposits may reveal the shape of a long-wavelength component of dynamic topography. Such a datum would provide a fundamental constraint on models of mantle convection[2,3]. □

Received 13 October 1989; accepted 23 February 1990.

1. Wise, D. U. in *The Geology of Continental Margins* (eds Burk, C. A. & Drake, C. L.) 45–58 (Springer, New York, 1974).
2. Hager, B. H., Clayton, R. W., Richards, M. A., Comer, R. P. & Dziewonski, A. M. *Nature* **313,** 541–545 (1985).
3. Hager, B. H. & Clayton, R. W. in *Mantle Convection* (ed. Peltier, R. W.) 657–763 (1989).
4. Hays, J. D. & Pitman, W. C. *Nature* **246,** 18–22 (1973).
5. Kominz, M. A. *Am. Ass. Petrol. Geol. Mem.* **36,** 109–127 (1984).
6. Dziewonski, A. M. *J. geophys. Res.* **89,** 5929–5952 (1984).
7. Dziewonski, A. M. & Woodhouse, J. H. *Science* **236,** 37–48 (1987).
8. Cazenave, A., Souriau, A. & Dominh, K. *Nature* **340,** 54–57 (1989).
9. Cazenave, A., Dominh, K., Rabinowicz, M. & Ceuleneer, G. *J. geophys. Res.* **93,** 8064–8077 (1988).
10. Harrison, C. G. A., Miskell, K. J., Brass, G. W., Saltzman, E. S. & Sloan, J. L. *Tectonics* **2,** 357–377 (1983).
11. Algeo, T. J. & Wilkinson, B. H. *J. geol. Soc. London.* (in the press).
12. Harrison, C. G. A. *et al. Earth planet. Sci. Lett.* **54,** 1–16 (1981).
13. Anderson, D. L. *Nature* **297,** 391–393 (1982).
14. Gurnis, M. *Nature* **332,** 695–699 (1988).
15. Gurnis, M. *Geophys. Res. Lett.* (in the press).

ACKNOWLEDGEMENTS. This work was funded by a NSF Presidential Young Investigator Award. H. Pollack, M. Richards and B. Wilkinson provided helpful comments.

Iberian plate kinematics: a jumping plate boundary between Eurasia and Africa

S. P. Srivastava*, H. Schouten†, W. R. Roest*, K. D. Klitgord‡, L. C. Kovacs§, J. Verhoef* & R. Macnab*

* Geological Survey of Canada, Atlantic Geoscience Centre, Bedford Institute of Oceanography, Dartmouth, Nova Scotia, B2Y 4A2, Canada
† Department of Geology and Geophysics, Woods Hole Oceanographic Institution, Woods Hole, Massachusetts 02543, USA
‡ US Geological Survey, Woods Hole, Massachusetts 02543, USA
§ US Naval Research Laboratory, Washington, DC, 20375-5000, USA

THE rotation of Iberia and its relation to the formation of the Pyrenees has been difficult to decipher because of the lack of detailed sea-floor spreading data, although several models have been proposed[1–7]. Here we use detailed aeromagnetic measurements from the sea floor offshore of the Grand Banks of Newfoundland to show that Iberia moved as part of the African plate from late Cretaceous to mid-Eocene time, with a plate boundary extending westward from the Bay of Biscay. When motion along this boundary ceased, a boundary linking extension in the King's Trough to compression along the Pyrenees came into existence. Finally, since the late Oligocene, Iberia has been part of the Eurasian plate, with the boundary between Eurasia and Africa situated along the Azores–Gibraltar fracture zone.

The sea-floor spreading lineation pattern between the Azores and Charlie Gibbs fracture zones as obtained from the present survey and previous compilations[8–12] (Fig. 1) provides the primary input into a reanalysis of the plate kinematics for the Iberian plate. The continuation of anomaly 34 into the Bay of Biscay[13] indicates that Iberia was separating from Eurasia during the late Cretaceous. Analysis of sea-floor spreading anomaly patterns on the Iberian plate between the Azores–Gibraltar transform zone and King's Trough, in conjunction with the patterns south of the Azores–Gibraltar zone and on the west flank of the Mid-Atlantic Ridge[8,11] showed that Iberia was attached to Africa from chron M0 to 13 (that is, 118 to 37 Myr). Further analysis of these data and new data from the present aeromagnetic survey east of the Grand Banks shows that the northern plate boundary of Iberia was more complicated than the single plate boundary at King's Trough used in the past[6,8,11]. Examination of magnetic lineations from the west flank of the ridge which we rotated to the east using arbitrary poles of rotation (Fig. 2) indicates that the sea-floor spreading pattern on the eastern flank of the Mid-Atlantic Ridge can be divided